

DOI: <https://doi.org/10.15407/ugz2026.01.041>

Batur, M. O.

0000-0001-9284-8858,

Selbesoğlu, M. O.

0000-0002-1132-3978

Istanbul Technical University, Istanbul, Turkey

Investigating Volcanic Plume Dispersion and Ash Deposition Effects on Snow Albedo in Antarctica

UDC 551.521.14:551.217.2:551.324.24(99)(045)

Volcanic eruptions are significant contributors to atmospheric aerosols, affecting global climate by altering radiative forcing. In remote regions such as Antarctica, volcanic ash plumes from eruptions in the Southern Hemisphere have the potential to impact snow albedo, altering the region's energy balance. This paper investigates the dispersion of volcanic ash from South American volcanoes over Antarctica using the HYSPLIT model and examines the effects of ash deposition on snow albedo using the SNICAR-Adv3 model. The study simulates various eruption scenarios and assesses how changes in snow's optical properties, such as albedo, are influenced by different levels of volcanic ash deposition. The findings demonstrate that ash deposition is most significant in the lower atmosphere (0–4000 m) due to gravitational settling and proximity to the surface, with air concentrations decreasing with altitude. It was found that snow albedo could potentially decrease by 1% due to volcanic ash deposition. The results suggest that while plume dispersion and ash deposition over Antarctica are plausible under specific atmospheric conditions, the extent of ash's impact on albedo varies significantly. This variability could accelerate snowmelt, influencing the Antarctic climate system and potentially altering the regional energy balance.

Keywords: *Antarctica; Antarctic Climate; Snow Albedo; Albedo Changes; Volcanic Ash Dispersion; Hypothetical Volcanic Eruption.*

Introduction

Volcanic eruptions are known to play a significant role in shaping global ecosystems and climate systems. They can cause temporary shifts in climate, often leading to cooling effects that last from a few years to even decades, depending on the magnitude of the eruption. Large-scale volcanic events release vast amounts of aerosols, such as sulfur dioxide, into the stratosphere, which reduces incoming solar radiation and triggers global cooling [1–2]. While these aerosols contribute to global temperature reductions, especially over oceans and ice-covered regions like Antarctica, their effects can be complex and regionally varied. For instance, studies following the 1991 eruption of Mt. Pinatubo documented significant cooling of the Southern Ocean, yet simulta-

neous warming of up to 0.8°C was observed along the Antarctic Peninsula [3–5]. This demonstrates the complexity of volcanic impacts, particularly in sensitive polar environments where warming could heighten the vulnerability of ice sheets and glaciers. Antarctica, the most remote continent on Earth, plays a critical role in regulating global climate and sea levels. Volcanic ash deposition in the region, though often limited due to the natural barriers posed by the Antarctic Circumpolar Current, can nonetheless occur through long-range atmospheric transport [6]. Over the past two decades, satellite remote sensing data have revealed trends in snow cover across East and West Antarctica, showing dynamic changes in the region's cryosphere that could be further exacerbated by external factors

For citation:

Batur, M. O., & Selbesoğlu, M. O. (2026). Investigating Volcanic Plume Dispersion and Ash Deposition Effects on Snow Albedo in Antarctica. *Ukrainian Geographical Journal*, 1, 41–54. [in English]. DOI: <https://doi.org/10.15407/ugz2026.01.041>

Copyright © 2026 Publishing House *Akadempyodyka* of the National Academy of Sciences of Ukraine.



The article is published under the open access license CC BY-NC-ND license

<https://creativecommons.org/licenses/by-nc-nd/4.0/>

such as volcanic ash deposition [7]. These changes, combined with the transport mechanism known as global distillation, can carry pollutants and ash particles over great distances, contributing to their accumulation in polar regions [8]. Volcanic ash, a key component of these pollutants, has the potential to disturb the delicate radiative balance of the Antarctic ice sheet by altering surface albedo—the fraction of solar energy reflected by the snow and ice. Even small changes in albedo can have pronounced effects on the region's energy balance, accelerating snowmelt and influencing local climate patterns. Several studies have focused on the transport of volcanic ash over long distances and its environmental impact. [9] analyzed the long-range dispersion of ash from the Sangay volcano in Ecuador, while research following the 2010 Eyjafjallajökull eruption in Iceland revealed significant ash deposition across Europe [10–11]. Some previous studies have demonstrated the potential for volcanic eruptions in South America, particularly those in the Andean Volcanic Arc, to influence the Antarctic region through long-range atmospheric transport of ash and aerosols. Tephra and sulfate layers identified in Antarctic ice cores have been linked to major eruptions, such as those from Mount Hudson in 1991, Lascar, and Quizapu in 1932, confirming interhemispheric dispersion under favorable meteorological conditions, including prevailing westerlies and cyclonic systems [12–14]. These findings highlight the capacity of explosive volcanic events in southern South America to alter Antarctic atmospheric composition and contribute to surface deposition, as evidenced by geochemical signatures in ice cores [14–15]. Such impacts underscore the need for continued research into ash plume trajectories and their environmental consequences to better understand the climatic implications of volcanic activity on polar regions [16]. Some satellite-based studies have also confirmed ash transport over vast distances, such as during the 2015 Calbuco eruption, which affected the ozone layer above Antarctica [17–18]. There is still a limited understanding of the impact of volcanic ash on Antarctic albedo and subsequent climatic effects. This study seeks to address this gap by simulating volcanic plume dispersion and ash deposition in Antarctica and assessing the potential impacts on snow albedo. Specifically, we aim to investigate the plausibility of volcanic ash from South American eruptions reaching the Antarctic continent and to evaluate the extent to which such deposition could

reduce snow albedo, potentially accelerating snowmelt and influencing local climate systems. To achieve this, we conduct forward-trajectory analyses using meteorological data from past years and model different volcanic eruption scenarios to track ash dispersion and deposition patterns. Additionally, we assess how variations in ash concentration and deposition rates at different altitudinal levels influence surface albedo, contributing to broader discussions on the radiative and climatic implications of volcanic activity in polar regions. This work provides a novel perspective on the environmental impact of volcanic eruptions in Antarctica, offering insights into the mechanisms of ash transport and deposition and their effects on snow albedo. Given the continent's critical role in global climate regulation, understanding the potential for volcanic ash to disrupt the surface energy balance in Antarctica is essential for predicting future climate scenarios, especially as the region becomes increasingly vulnerable to external disturbances like volcanic eruptions.

Area description and methodology

Volcanic activity in South America

The Andean Volcanic Arc, formed by the subduction of the Nazca tectonic plate beneath the South American plate, spans the South American coast, cutting through Argentina, Bolivia, Chile, Colombia, Ecuador, and Peru (**Figure 1**). This subduction process fuels volcanic activity, creating a complex volcanic belt that exhibits a diverse range of eruption styles and morphologies [19]. Simultaneously, the Pacific Ring of Fire, which encircles the Pacific Ocean, is a global manifestation of tectonic movements, marked by numerous volcanic arcs.

The Andean Volcanic Arc unfolds in four primary volcanic zones, separated by significant volcanic gaps [20]. The Northern Volcanic Zone stretches from Colombia to Ecuador, encompassing all continental volcanoes in this region. Ecuador alone hosts 55 volcanoes, which pose significant hazards to densely populated areas, including prominent volcanoes such as Galeras and Nevado del Ruiz. The Central Volcanic Zone extends from Peru to Chile, containing 44 major and 18 minor volcanic centers.

Further south, the Southern Volcanic Zone spans over 1,400 km, from central Chile to the Aysen Region, comprising at least 60 historically and potentially active volcanic edifices, along with numerous

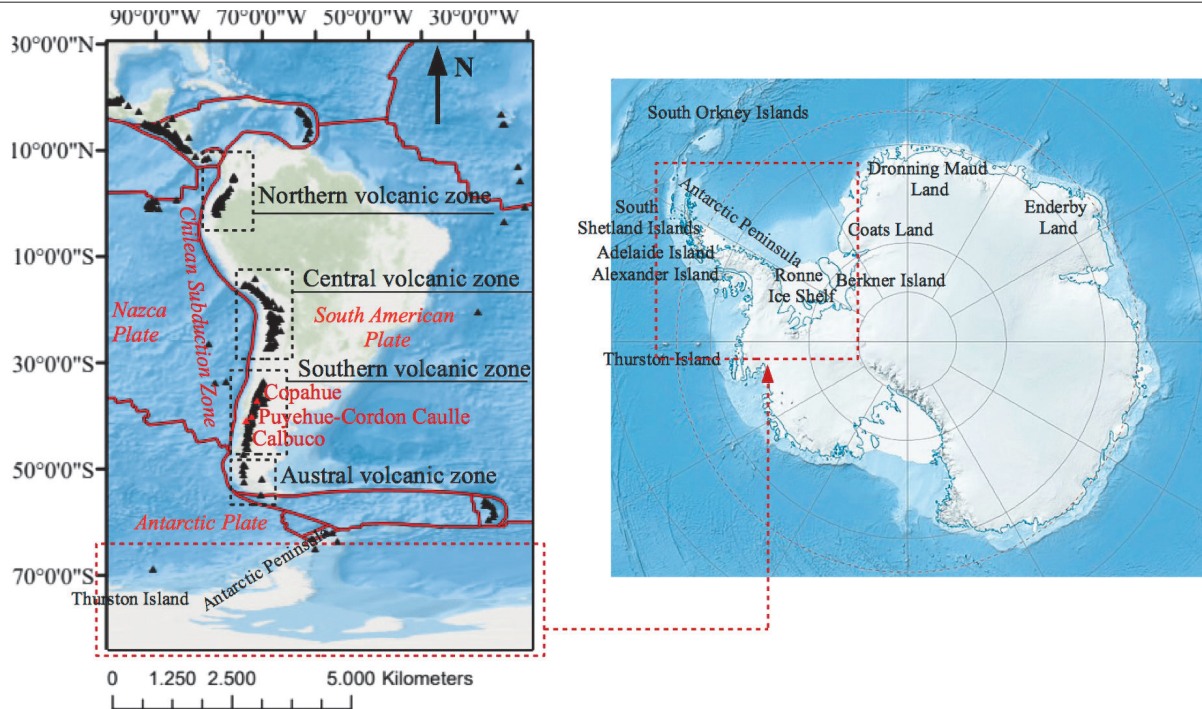


Fig. 1. Schematic map of South America and the Pacific oceanic plates along with the geographical location of volcanoes.

minor eruptive centers. This zone culminates at the Chile Triple Junction, triggering the Patagonian Volcanic Gap and transitioning into the Austral Volcanic Zone, which stretches over 965 km. The Patagonian Volcanic Gap, occurring between 46° S and 49° S, is so named because no seismic activity is detected beneath this area. The Austral Volcanic Zone consists of five stratovolcanoes and a small complex of Holocene domes.

According to the Global Volcanism Program [21], 44 volcanoes in Chile have erupted at least once since 1820, with 15 of these erupting within the last 20 years. The most historically active volcanoes in Chile are Copahue, Puyehue-Cordon Caulle, and Calbuco (Figure 1). These volcanoes are highly active and known for large, explosive eruptions that produce thick layers of lava, volcanic ash, and SO₂ emissions. Calbuco has an eruption frequency of approximately 19 years [22], while Copahue has erupted ten times since 1900, and Puyehue has recorded nine eruptions since 1900 [23].

Figure 1 also depicts a map of Antarctica, highlighting its key geographical features. The red dotted lines outline the western portion of Antarctica, particularly the Antarctic Peninsula and surrounding islands, which are the closest areas to South America. These regions are potentially vulnerable to volcanic pollution due to their proximity.

Volcanic selection

According to the U. S. Geological Survey (USGS), volcanic eruptions are classified into 11 types based on magma composition and eruption characteristics:

- (1) mafic magmas with a standard eruption (M0);
- (2) mafic magmas with a small eruption (M1);
- (3) mafic magmas with a medium eruption (M2);
- (4) mafic magmas with a large eruption (M3);
- (5) silicic magmas with a standard eruption (S0);
- (6) silicic magmas with a small eruption (S1);
- (7) silicic magmas with a medium eruption (S2);
- (8) silicic magmas with a large eruption (S3);
- (9) co-ignimbrite cloud (S8);
- (10) brief silicic eruptions (S9); and
- (11) submarine eruptions (U0) [24].

To assess the potential arrival of volcanic plumes in Antarctica, several volcanoes were selected based on specific criteria:

- (1) proximity to Antarctica, specifically volcanoes located within 3,000–4,000 km of the Antarctic Peninsula;
- (2) eruptive history, including volcanoes with at least one explosion within the last 50 years; and
- (3) eruption type, ensuring a variety of magma types. Based on these criteria, three volcanoes in Chile were selected.

Table 1. Brief information on selected volcanoes

Volcano name	Calbuco	Copahue	Puyehue Cordon Caulle
Location	Lat 41.33° S Lon 72.61° W	Lat 37.85° S Lon 71.18° W	Lat 40.59° S Lon 72.11° W
Primary volcano type	Stratovolcano	Stratovolcano	Stratovolcano
Summit, m	1,974	2,953	2,236
Elevation, km	1.9738	2.9529	2.2360
Last emission	2015 Apr 22	2012 Dec 22	2011 Jun 04

Table 2. The values of HYSPLIT input data for the simulation of volcanic ash

HYSPLIT input parameters	Calbuco eruption	Copahue eruption	Puyehue Cordon Caulle eruption
Plume height, km	11	5	11
Eruption duration, hr	3	12	3
Mass eruption rate, kg/s	4×10^6	2×10^5	4×10^6
Erupted volume, km ³	0.015	0.003	0.015
Mass fraction of fine ash	0.4	0.1	0.4
Eruption type	S2	S1	S0

Table 1 provides an overview of the key characteristics of these volcanoes, along with details of their most recent eruptions.

HYSPLIT trajectory and ash dispersion model

To estimate the trajectory of air particles reaching Antarctica and to simulate the volcanic eruption, both forward trajectory analysis and dispersion modeling were conducted using the Hybrid Single-Particle Lagrangian Integrated Trajectory (HYSPLIT) model. Developed by the National Oceanic and Atmospheric Administration (NOAA) Air Resources Laboratory and the Australian Bureau of Meteorology Research Center, HYSPLIT has been widely used in atmospheric transport and dispersion studies. Its applications include sand and dust modeling [25], simulation of radioactive releases [26], ensemble forecasting of wildfires [27], and volcanic ash deposition modeling [28], among others.

HYSPLIT's name reflects its use of both Lagrangian and Eulerian approaches. In fluid mechanics, the Lagrangian method focuses on tracking individual particles and calculating their trajectories, while the Eulerian method deals with the overall concentration of particles, calculating their diffusion and convection. The combination of these two approaches allows for a more comprehensive analysis of particle-fluid interactions [29].

In this study, forward trajectories were initiated from the volcanic sites to determine the likelihood of volcanic ash reaching Antarctica. Additionally, an atmospheric dispersion model simulated the spatiotemporal behavior of the volcanic ash plumes. To establish when ash could reach Antarctica, multiple forward trajectories were calculated over time intervals ranging from 3 to 72 hours.

The HYSPLIT model was driven by meteorological data from the Global Data Assimilation System (GDAS), using hourly archived data at 1° by 1° resolution. For volcanic ash modeling, the input parameters were based on eruption source parameters provided by the USGS. The USGS assigns eruption characteristics, such as column height, eruption duration, mass eruption rate, eruption volume, and the percentage of fine ash, for each volcano [24]. **Table 2** provides the key input parameters used in the HYSPLIT simulations.

Volcanic ash concentrations were calculated for different atmospheric heights since meteorological conditions vary with altitude, affecting the ash's spatial distribution. Upon running the HYSPLIT model, we obtained forward trajectory data and ash plume concentration maps, which helped visualize the ash's movement and concentration over time.

Albedo calculations

We developed a MATLAB code to calculate the change in snow albedo due to volcanic ash deposition by iterating over various snow physical prop-

erties (snow depth, grain radius, and snow density), optical properties of volcanic ash (single-scattering albedo (SSA) and asymmetry factor), and ash deposition values across a range of wavelengths. This calculation is based on a simplified radiative transfer model adapted from the Snow, Ice, and Aerosol Radiative Model (SNICAR) framework, which is widely used for simulating the interaction of solar radiation with snow packs.

SNICAR calculates snow albedo based on a combination of snow's physical properties and the optical properties of impurities such as volcanic ash or black carbon [30]. It is particularly useful for assessing the impact of these contaminants on snow reflectivity and climate. SNICAR incorporates the detailed physics of light scattering and absorption within snow, considering both the intrinsic properties of snow grains and the external contaminants mixed into the snowpack [31].

The snow albedo, denoted as α , is calculated using a radiative transfer equation based on the two-stream approximation (1) [32]:

$$\alpha = (1 - w_{\text{combined}}) e^{-(\tau_{\text{snow}} + \tau_{\text{ash}})} + w_{\text{combined}} (1 - g_{\text{combined}}) \left(1 - e^{-(\tau_{\text{snow}} + \tau_{\text{ash}})}\right) \mu \quad (1)$$

where α is the snow albedo, w_{combined} is the combined SSA of snow and ash; τ_{snow} and τ_{ash} are the optical depths of snow and volcanic ash, respectively, g_{combined} is the combined asymmetry factor of snow and ash, and μ is the cosine of the solar zenith angle.

The optical depth represents how much light is attenuated as it passes through a medium. For snow and volcanic ash, optical depth depends on physical properties such as snow depth, grain radius, and ash deposition. The optical depth for snow, τ_{snow} , is given by (2):

$$\tau_{\text{snow}} = \frac{D \times \rho_{\text{snow}}}{r} \quad (2)$$

where D is the snow depth (m), r corresponds to the snow grain radius (m), and ρ_{snow} is the snow density (kg/m^3).

The optical depth of volcanic ash, τ_{ash} , depends on the ash deposition rate M_{ash} and the SSA w_{ash} of the ash particles. It is given by equation (3):

$$\tau_{\text{ash}} = M_{\text{ash}}(1 - w_{\text{ash}}). \quad (3)$$

Two key optical properties govern light scattering in the snow-ash mixture: the SSA w and the

asymmetry factor g . The SSA represents the fraction of light that is scattered rather than absorbed by a particle. For snow and ash, their combined SSA w_{combined} is calculated as the average of their respective values and is given by equation (4):

$$w_{\text{combined}} = \frac{w_{\text{snow}} + w_{\text{ash}}}{2} \quad (4)$$

where w_{snow} is typically 0.9, and w_{ash} varies between 0.6 and 0.9.

The asymmetry factor g_{combined} , which describes whether light is mostly scattered forward or backward, is calculated similarly by equation (5):

$$g_{\text{combined}} = \frac{g_{\text{snow}} + g_{\text{ash}}}{2} \quad (5)$$

where g_{snow} is 0.85, and g_{ash} varies between 0.7 and 0.9.

To evaluate the impact of varying parameters on snow albedo, the percentage change is computed using equation (6):

$$\Delta\alpha = \frac{\alpha_{\text{new}} - \alpha_{\text{base}}}{\alpha_{\text{base}}} \times 100\% \quad (6)$$

where α_{new} is the albedo calculated for a new set of parameters (e.g., higher ash deposition or larger grain size), α_{base} is the base albedo under clean snow conditions.

Sensitivity analysis

To quantify the impact of volcanic ash deposition on snow albedo, we conducted a comprehensive sensitivity analysis by examining a wide range of ash deposition rates and snow physical properties. Snow albedo is influenced by various factors, including grain size, snow depth, snow density, and optical properties such as SSA and the asymmetry factor. Our analysis sought to understand how varying ash deposition levels alter snow albedo compared to clean snow conditions.

The calculations were based on a radiative transfer model using the SNICAR framework. The analysis followed these steps:

1. Base Case Scenario: We first established a base scenario representing typical Antarctic conditions. The snow depth was set to 1 meter, the grain size was fixed at 100 μm , and the snow density was assumed to be 200 kg/m^3 . For the volcanic ash, we used an SSA of 0.75 and an asymmetry factor of 0.8. Using these values, the base albedo was calculated for clean snow using a radiative transfer

function, which incorporates both the single scattering albedo and asymmetry factor of snow and ash particles.

2. Ash Deposition Sensitivity: Ash deposition levels were varied logarithmically from 0.1 mg/m² to 10,000 mg/m² to capture different scenarios of volcanic activity. For each ash deposition level, we recalculated the snow albedo using the radiative transfer model, allowing us to estimate the reduction in albedo as the ash concentration increased.

3. Snow Properties Sensitivity: We then performed a sensitivity analysis for snow depth (0.5 m to 2 m), grain size (50 μm to 200 μm), and snow density (100 kg/m³ to 500 kg/m³). By systematically varying these parameters, we recalculated the albedo for each combination and compared it to the base case. This allowed us to quantify the sensitivity of snow albedo to these physical properties.

4. Optical Properties Sensitivity: Finally, we analyzed how changes in the optical properties of volcanic ash influence snow albedo. The SSA of the ash was varied from 0.6 to 0.9, and the asymmetry factor was adjusted from 0.7 to 0.9. For each combination of SSA and asymmetry factor, we recalculated the albedo and computed the percentage change compared to the base albedo.

Sensitivity analysis for snow properties are calculated using equations (7)–(9):

Snow depth sensitivity (7):

$$\Delta\alpha_{\text{depth}} = \frac{\alpha(D, r_{\text{base}}, \rho_{\text{base}}, M_{\text{ash}}, w_{\text{ash}}, g_{\text{ash}}) - \alpha_{\text{base}}}{\alpha_{\text{base}}} \times 100\% \quad (7)$$

where $\alpha(D, r_{\text{base}}, \rho_{\text{base}}, M_{\text{ash}}, w_{\text{ash}}, g_{\text{ash}})$ is the snow albedo calculated with the modified snow depth D , while keeping the other parameters constant (grain radius r_{base} , snow density ρ_{base} , ash deposition M_{ash} , ash SSA w_{ash} , and ash asymmetry factor g_{ash}).

Grain radius sensitivity (8):

$$\Delta\alpha_{\text{grain}} = \frac{\alpha(D_{\text{base}}, r, \rho_{\text{base}}, M_{\text{ash}}, w_{\text{ash}}, g_{\text{ash}}) - \alpha_{\text{base}}}{\alpha_{\text{base}}} \times 100\% \quad (8)$$

where $\alpha(D_{\text{base}}, r, \rho_{\text{base}}, M_{\text{ash}}, w_{\text{ash}}, g_{\text{ash}})$ is the snow albedo calculated with a modified snow grain radius r , while keeping the other parameters constant.

Snow density sensitivity (9):

$$\Delta\alpha_{\text{density}} = \frac{\alpha(D_{\text{base}}, r_{\text{base}}, \rho_{\text{snow}}, M_{\text{ash}}, w_{\text{ash}}, g_{\text{ash}}) - \alpha_{\text{base}}}{\alpha_{\text{base}}} \times 100\% \quad (9)$$

where $\alpha(D_{\text{base}}, r_{\text{base}}, \rho_{\text{snow}}, M_{\text{ash}}, w_{\text{ash}}, g_{\text{ash}})$ is the snow albedo calculated with a modified snow density ρ_{snow} , while keeping the other parameters constant.

Sensitivity analysis for optical properties are calculated using equations (10)–(11):

SSA sensitivity (10):

$$\Delta\alpha_{\text{SSA}} = \frac{\alpha(D_{\text{base}}, r_{\text{base}}, \rho_{\text{base}}, M_{\text{ash}}, w_{\text{ash}}, g_{\text{ash}}) - \alpha_{\text{base}}}{\alpha_{\text{base}}} \times 100\% \quad (10)$$

where $\alpha(D_{\text{base}}, r_{\text{base}}, \rho_{\text{base}}, M_{\text{ash}}, w_{\text{ash}}, g_{\text{ash}})$ is the snow albedo calculated with a modified SSA of volcanic ash w_{ash} , while keeping the other parameters constant.

Asymmetry factor sensitivity (11):

$$\Delta\alpha_g = \frac{\alpha(D_{\text{base}}, r_{\text{base}}, \rho_{\text{base}}, M_{\text{ash}}, w_{\text{base}}, g_{\text{ash}}) - \alpha_{\text{base}}}{\alpha_{\text{base}}} \times 100\% \quad (11)$$

where $\alpha(D_{\text{base}}, r_{\text{base}}, \rho_{\text{base}}, M_{\text{ash}}, w_{\text{base}}, g_{\text{ash}})$ is the snow albedo calculated with a modified asymmetry factor g_{ash} , while keeping the other parameters constant.

Results

Pathway transport of volcanic ashes

Table 3 summarizes the forward trajectory simulations generated using the HYSPLIT model for each month of a hypothetical volcanic eruption. The table presents the dominant transport directions, dispersion characteristics, and trajectory behavior, allowing identification of periods when volcanic ash is more likely to reach Antarctic regions.

The results demonstrate a clear seasonal influence on ash dispersion patterns. According to the summarized trajectory characteristics, months such as February, June, July, August, and September are associated with transport directions and dispersion patterns that favor southward movement toward Antarctic regions. These months are characterized by wider dispersion, increased trajectory curvature, and more variable atmospheric conditions, indicating a higher probability of ash reaching Antarctica.

Table 3. Summary of forward trajectory patterns derived from HYSPLIT simulations for each month, including dominant transport direction, dispersion characteristics, and trajectory behavior

Month	Dominant direction	Dispersion pattern	Relative spread	Trajectory behavior	General interpretation
December	NE-E	Moderately curved	Medium	Consistent flow	Stable atmospheric transport
January	E-SE	Slightly diverging	Medium	Smooth trajectories	Moderate variability
February	SE	Strong divergence	Wide	Curved	Increased dispersion influence
March	E-NE	Mixed	Medium	Semi-stable	Transitional pattern
April	E	Parallel	Narrow-medium	Linear	More stable flow regime
May	SE-S	Divergent	Wide	Strong curvature	Enhanced atmospheric
June	Variable E-W	Highly dispersed	Very wide	Irregular	Unstable atmospheric conditions
July	SE	Moderately focused	Medium	Slight curvature	Controlled dispersion
August	E-SE	Diverging	Medium-wide	smooth	Seasonal transition
September	NE-E	moderate	medium	Semi-linear	Stabilizing flow
October	E	Narrow	Low	Linear	Strong directional control
November	NE-N	Mixed	Medium	Curved	Variable atmospheric influence

Table 4. Summary of modeled volcanic ash dispersion at different altitude ranges for selected volcanoes, including concentration levels, spatial distribution, and dispersion characteristics

Volcano	Altitude range (m)	Relative concentration	Dispersion direction	Spatial extent	Pattern type
Calbuco	0–4,000	High near source	E-SE	Local-regional	Concentrated
Calbuco	4,000–6,000	Medium	E	Regional	Expanding
Calbuco	6,000–8,000	Lower	E-NE	Wide	Diffuse
Copahue	0–4,000	High	SE	Local	Concentrated
Copahue	4,000–6,000	Medium	SE-E	Regional	Expanding
Copahue	6,000–8,000	Low	E-NE	Wide	Diffuse
Puyehue-Cordon Caulle	0–4,000	Very high	E-SE	Regional	Dense plume
Puyehue-Cordon Caulle	4,000–6,000	Medium	E	Wide	Expanding
Puyehue-Cordon Caulle	6,000–8,000	Low-very low	E-NE	Very wide	Diffuse

In contrast, months such as March, April, May, and November exhibit more stable or predominantly eastward and westward transport patterns, limiting southward dispersion. These periods are characterized by narrower or more linear trajectories, suggesting a lower likelihood of ash transport toward Antarctic regions. Overall, the variability in dominant directions, spread, and trajectory behavior

highlights the strong influence of seasonal atmospheric circulation on ash dispersion.

Ash dispersion from simulated volcanic events

Table 4 summarizes the modeled volcanic ash dispersion 72 hours after hypothetical eruptions of three volcanoes: Calbuco, Copahue, and Puyehue-Cordón Caulle. The table presents disper-

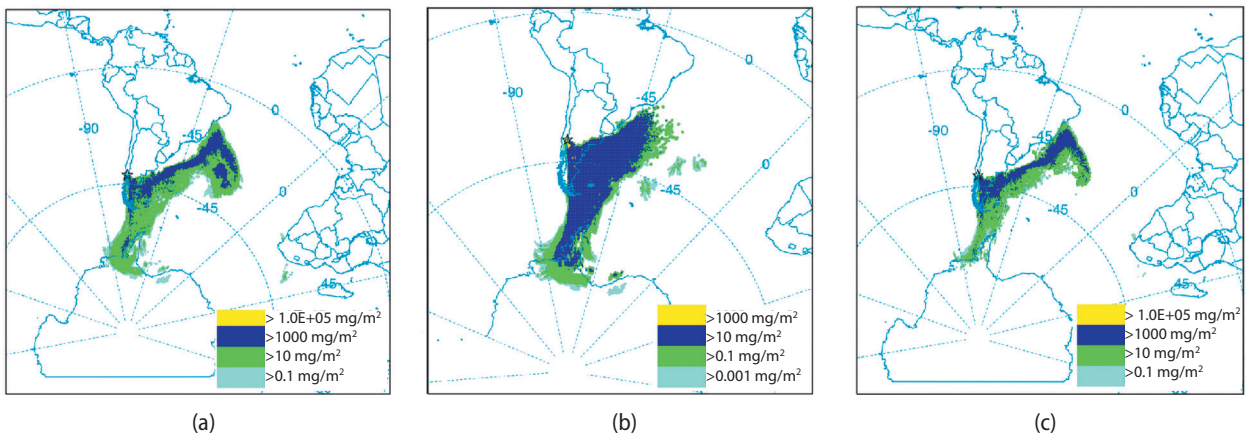


Fig. 2. Simulation results of volcanic ash deposition 72 hours after the hypothetical eruption: (a) Calbuco volcano; (b) Copahue volcano; (c) Puyehue-Cordón Caulle volcano.

sion characteristics across three altitude ranges (0–4,000 m, 4,000–6,000 m, and 6,000–8,000 m), including relative concentration levels, transport directions, and spatial extent of ash clouds.

The results indicate that ash concentrations are generally highest near the volcanic source and decrease with distance, reflecting progressive dispersion of the ash cloud. Across all volcanoes, lower altitude ranges (0–4,000 m) are characterized by more concentrated and spatially limited ash distributions, while higher altitudes show broader dispersion patterns and wider spatial coverage. This demonstrates the influence of atmospheric transport processes, where ash particles become increasingly dispersed at higher elevations. Comparative analysis of the three volcanoes shows that eruptions of Calbuco and Puyehue-Cordón Caulle produce similar levels of ash dispersion toward Antarctic regions, with concentrations ranging approximately from 0.0001 mg/m^3 to 0.01 mg/m^3 . In contrast, Copahue exhibits slightly lower concentrations, reaching values from approximately 0.000001 mg/m^3 to 0.01 mg/m^3 , indicating a relatively weaker impact under the modeled conditions. The vertical distribution patterns further reveal that ash concentrations remain relatively consistent between the 4,000 m and 6,000 m altitude ranges, suggesting stable transport within these atmospheric layers. At higher altitudes (6,000–8,000 m), a slight decrease in concentration is observed, indicating enhanced dispersion and possible settling of ash particles.

Ash deposition patterns from simulated volcanic events

Figure 2 presents ground ash deposition maps for three different volcanoes, illustrating how pollutants

from volcanic eruptions settle onto the Earth's surface. These maps provide a visual representation of the spatial distribution of volcanic ash deposition, with varying intensities indicated by color gradients.

When interpreting these maps, it's essential to start by examining the map legend, which details the pollution levels. In the Antarctic regions, the highest detected level of ash deposition exceeds 10 mg/m^2 , indicating significant environmental impact in these areas.

Looking at **Figure 2a**, which depicts ash deposition from the Calbuco volcano, we observe that the ash has spread over a vast area. High concentrations of ash (shown by blue color) are particularly prominent off the southern coast of South America and extend into the South Atlantic Ocean. This suggests that the hypothetical eruption could be influenced by wind patterns that carried the ash far from the volcano.

In **Figure 2b**, the ash deposition from the Copahue volcano is also widespread, but overall, the intensity of the ash deposition is lower compared to Calbuco. Although the highest concentrations (highlighted in yellow) are present, they are more concentrated near the eruption site, indicating that the ash did not spread as extensively as in the first map. This could be due to a combination of factors, including the strength of the eruption and local meteorological conditions at the time.

Finally, **Figure 2c** displays the ash deposition from the Puyehue-Cordon Caulle volcano, which exhibits a spatial distribution similar to the Calbuco eruption. Large areas are covered with high concentrations of ash, again particularly along the southern coast of South America and into the South Atlantic. While the overall pattern resembles that of Calbuco,

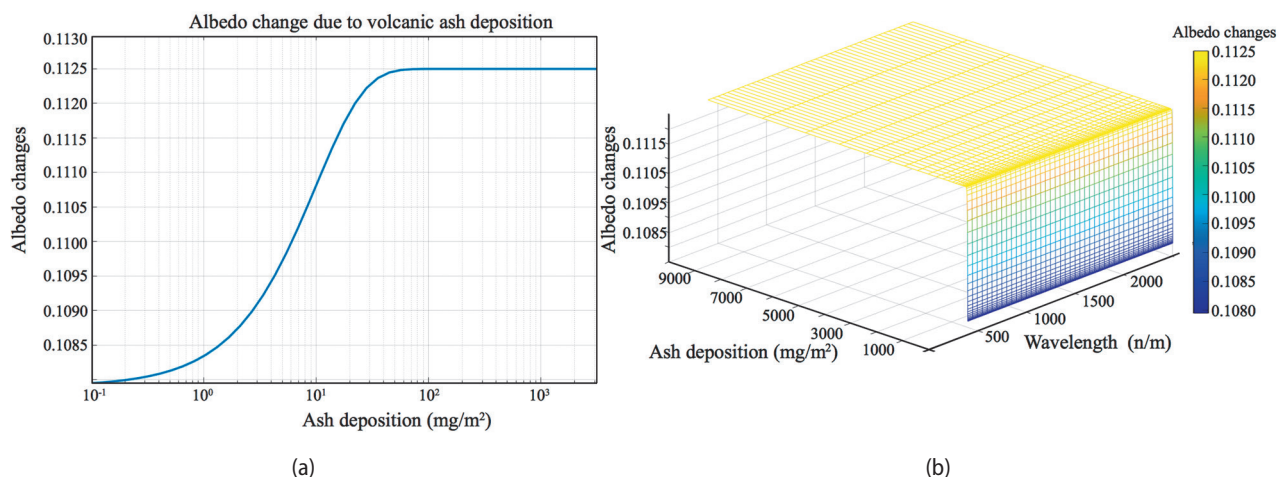


Fig. 3. Effects of volcanic ash deposition on snow surface albedo under different conditions
(a) Changes of albedo as a function of ash deposition; (b) Albedo changes across wavelengths and ash deposition.

there may be subtle differences in the intensity and extent of the ash spread, possibly due to differences in eruption dynamics or atmospheric conditions at the time.

Albedo changes

Figure 3 illustrates the impact of volcanic ash deposition on snow surface albedo under varying conditions.

Figure 3a presents the relationship between albedo and ash deposition. The X-axis represents ash deposition (in mg/m^2) on a logarithmic scale, ranging from very low ($0.1 \text{ mg}/\text{m}^2$) to very high levels ($10,000 \text{ mg}/\text{m}^2$). The Y-axis shows the albedo, or the snow's reflectivity, where higher values indicate more reflective surfaces and lower values represent increased absorption of solar radiation. At minimal ash deposition levels (around $0.1 \text{ mg}/\text{m}^2$), snow retains a relatively high albedo, reflecting most incoming solar radiation. As ash deposition increases, the albedo decreases because the dark volcanic ash particles accumulate on the snow surface, absorbing more sunlight and reducing reflectivity.

Figure 3b shows how albedo varies across different wavelengths and ash deposition levels. The X-axis represents light wavelengths (ranging from 400 nm to 2,500 nm), which covers the visible and near-infrared portions of the spectrum. The Y-axis shows the ash deposition, and the Z-axis represents albedo, which changes based on the wavelength and the amount of ash. As ash deposition increases, albedo decreases across all wavelengths, with the effect being particularly strong in the visible light range, where clean snow is highly reflective. The reduction in albedo is more pronounced at lower ash deposi-

tion levels. However, beyond a certain deposition threshold, further increases in ash have a diminishing impact on reflectivity, indicating a saturation effect. This suggests that once the snow surface is sufficiently covered by ash, additional ash deposition has a smaller incremental effect on reducing albedo. This non-linear relationship highlights that small amounts of ash can significantly lower albedo initially, but the effect plateaus as deposition increases.

The Pearson correlation coefficient between ash deposition values and snow albedo was calculated to be 0.3882, with a p -value of 0.005341. This result is statistically significant at the $p < 0.05$ level. The coefficient of 0.3882 suggests a moderate positive correlation, indicating that as ash deposition increases, there is a tendency for snow albedo to decrease. The statistically significant p -value implies that this relationship is unlikely to be due to random chance, confirming that volcanic ash deposition has a measurable impact on snow albedo.

Albedo sensitivity results

To evaluate how various physical parameters influence snow albedo, a sensitivity analysis was conducted on four key variables: snow depth, snow grain radius, snow density, and snow optical properties. **Figure 4** illustrates the results of sensitivity analysis.

Figure 4a illustrates the sensitivity of albedo to snow depth. Results indicate that shallow snow ($\leq 0.5 \text{ m}$) increases albedo by more than 1%, likely due to enhanced reflectivity from the underlying snowpack. However, as snow depth increases beyond 1 m, the change becomes negative, suggesting a diminishing albedo effect, possibly due to light absorption in deeper layers.

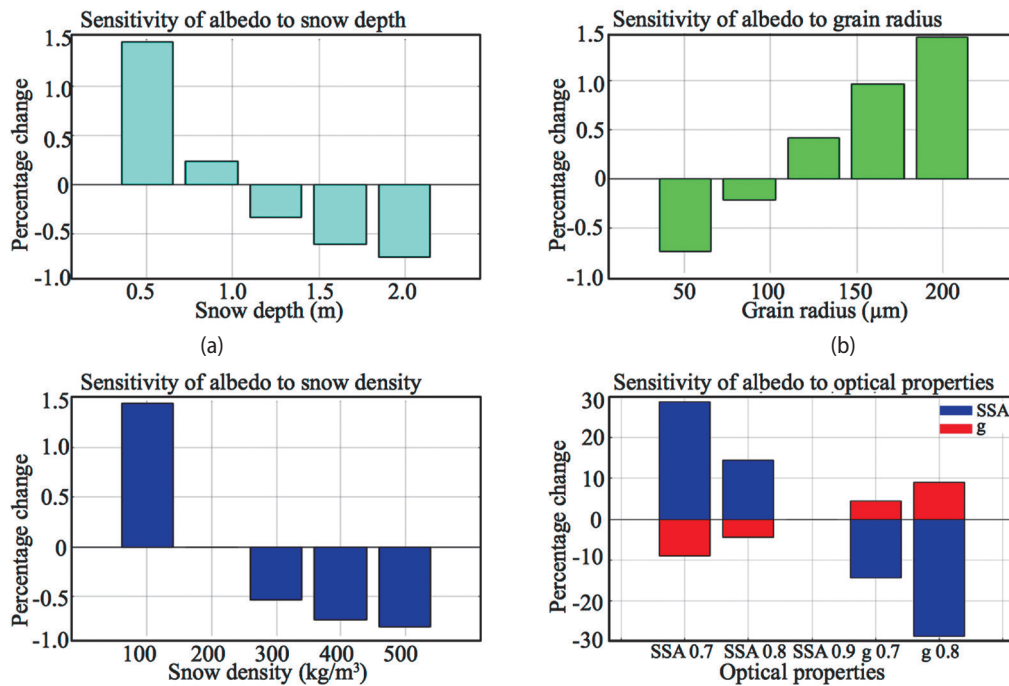


Fig. 4. Albedo sensitivity analysis: (a) sensitivity of albedo to snow depth; (b) sensitivity of albedo to grain radius; (c) sensitivity of albedo to snow density; (d) sensitivity of albedo to optical properties.

Figure 4b presents the response of albedo to varying snow grain radius. An increase in grain size from 50 μm to 200 μm leads to a progressive and significant reduction in albedo, with the smallest grains causing a decrease of over 1%. Larger grain sizes absorb more radiation, reducing surface reflectivity, making this a critical factor for albedo modeling.

Figure 4c shows the sensitivity of albedo to snow density. At lower densities (~100 kg/m³), albedo increases by over 1.5%. Conversely, increasing the density beyond 300 kg/m³ results in a notable decrease in albedo. This outcome reflects the transition from fresh, fluffy snow to compacted snow, which has a reduced scattering ability due to lower air content.

Finally, **Figure 4d** explores the influence of optical properties, specifically the snow specific surface area (SSA) and single-scattering albedo (*g*). A decrease in SSA or an increase in the asymmetry parameter (*g*) causes substantial reductions in albedo that is up to nearly 30% in some combinations.

Discussion

Relationship between ash deposition and air concentration at different altitudinal levels

The analysis of volcanic ash dispersion revealed a distinct relationship between ash deposition rates

and air concentration at varying altitudinal bands (between 0 m and 4000 m, between 4000 m and 6000 m, and between 6000 m and 8000 m). In the lower atmosphere (0–4000 m), ash concentration was relatively higher compared to upper levels due to gravitational settling and proximity to the surface. This increased deposition is directly linked to the denser ash plume, which is more affected by gravity and air drag, resulting in a larger amount of ash reaching the ground in this range. Between 4000–6000 m, a transition phase was observed where air concentration of ash decreased slightly, but still contributed significantly to the deposition. The mid-level atmosphere is characterized by lower vertical mixing and weaker updrafts, leading to a modest accumulation of ash particles. Finally, at the 6000–8000 m level, air concentration of volcanic ash dropped substantially due to reduced particulate matter density and the longer timescales required for ash particles to settle from such heights. Nevertheless, particles from this altitude still contributed to the overall deposition, albeit at much lower rates. This indicates that the primary ash deposition in Antarctica is influenced by air concentration at lower levels (0–4000 m), whereas ash from higher altitudes tends to disperse more broadly, contributing to distant deposition through long-range transport.

Impact of volcanic ash on snow albedo

This study revealed that volcanic ash deposition caused a measurable reduction in snow albedo, with a 1% decrease in reflectivity observed across affected regions. Volcanic ash, consisting of dark-colored particulate matter such as silicates and oxides, settles on the snow surface and absorbs more incoming solar radiation compared to pristine snow, which typically exhibits a high albedo of up to 90% in the visible spectrum [33–34]. Although a 1% reduction in albedo appears minor, it has significant localized and broader climatic implications due to the high sensitivity of snow-covered surfaces to changes in reflectivity. The darkening of snow by ash increases the absorption of solar radiation, with even small albedo reductions leading to substantial increases in surface energy uptake. For instance, under typical Antarctic summer conditions with incoming solar radiation of approximately 300 W/m², a 1% albedo reduction translates to an additional 3 W/m² of absorbed energy, sufficient to initiate or accelerate snowmelt [35–36]. This enhanced absorption raises surface temperatures, promoting grain coarsening in the snowpack, which further reduces albedo and amplifies melting [37].

In regions with concentrated ash deposition, such as near the Antarctic Peninsula, the snow surface absorbs significantly more solar radiation, leading to accelerated melting and modifications to the surface energy balance. The persistence of volcanic ash on the snow surface, influenced by factors such as wind redistribution, precipitation, and subsequent snowfall events, can prolong these effects, contributing to sustained albedo reduction over weeks to months [38]. As ash particles mix into the snowpack through meltwater percolation or wind-driven burial, they become more effective at absorbing solar radiation, as subsurface ash continues to darken the snow even after new snow accumulation [39]. This mixing process can lead to a cumulative albedo reduction, exacerbating the climatic impact over time. Studies of analogous impurities, such as black carbon, indicate that even low concentrations of light-absorbing particles (on the order of ng/g) can reduce snow albedo by 1–2%, with measurable effects on regional snowmelt rates [40]. The findings of this study align with these observations, underscoring that a 1% albedo reduction from volcanic ash is not trivial and can drive significant environmental changes in Antarctica's sensitive cryospheric system.

Radiative and climatic implications

The radiative impact of ash deposition, as observed in this study, influences regional climate patterns, particularly in sensitive polar environments like Antarctica. Increased absorption of solar radiation may alter local temperature profiles, potentially affecting ice dynamics, ocean-atmosphere interactions, and contributing to the long-term acceleration of ice sheet melting. These effects are consistent with research highlighting the sensitivity of Antarctic ice sheets to surface albedo changes, which can exacerbate mass loss and contribute to global sea-level rise [41–42]. Given the critical role of Antarctica in global sea-level regulation, our results align with studies emphasizing that even minor changes in snow and ice albedo from impurities like volcanic ash can have cascading effects on global climate systems [43–44].

Furthermore, volcanic ash in the atmosphere affects radiative forcing by both scattering and absorbing solar radiation, which can lead to short-term cooling effects globally, depending on the scale of the eruption [45]. However, the localized deposition of ash on snow in polar regions, as this study demonstrates, tends to result in warming effects due to albedo reduction, a finding supported by research on volcanic aerosol impacts in polar environments [46]. This duality underscores the complex and regionally variable nature of volcanic eruptions' net climate impact, as noted in studies of past eruptions like Pinatubo and Calbuco [18]. Our research thus confirms and extends prior work, highlighting that a 1% albedo reduction from volcanic ash deposition is a significant driver of climatic change in Antarctica, with implications for regional and global climate dynamics.

Conclusion

This study investigated the effects of volcanic plume dispersion and ash deposition on snow albedo in Antarctica, highlighting key relationships between ash concentration at different altitudinal levels and the resulting impacts on surface reflectivity. The findings demonstrate that ash deposition is most significant in the lower atmosphere (0–4000 m) due to gravitational settling and proximity to the surface, with air concentrations decreasing with altitude. The deposition of volcanic ash resulted in a 1% reduction in snow albedo, a seemingly minor change with potentially substantial radiative and climatic consequences. This reduction leads to increased

absorption of solar radiation, accelerating snowmelt and contributing to positive feedback loops that may exacerbate local and regional warming. These processes have the potential to influence the stability of the Antarctic ice sheet and, consequently, global sea levels.

While this study offers valuable insights into the relationship between volcanic ash deposition and snow albedo, several avenues for future research can expand our understanding of the broader climatic and environmental implications:

1. Future studies should incorporate long-term observational data to monitor the persistence and evolution of ash on snow surfaces, accounting for factors such as wind redistribution, snowfall events, and ash mixing into the snowpack. Incorporating this data into high-resolution climate models would improve predictions of the long-term impacts of ash deposition on snowmelt and ice dynamics in Antarctica.

2. Future research could explore how variations in Antarctic climatic conditions (such as wind patterns, precipitation rates, and temperature fluctuations) influence the deposition and persistence of volcanic ash on snow and ice surfaces. These conditions may alter the extent to which ash particles affect snow albedo and the rate of snowmelt.

3. Impact on Antarctic Ice Dynamics: The interaction between volcanic ash deposition and Antarctic ice dynamics remains an open area of research. Studies should investigate how changes in snow albedo and increased meltwater generation impact the flow and stability of glaciers and ice sheets. Understanding these processes is critical for predicting future contributions to global sea-level rise.

4. Global Climatic Impacts: Expanding the scope of research to assess the interplay between local albedo changes in polar regions and global climate dynamics would provide a more comprehensive understanding of how volcanic ash deposition in Antarctica contributes to worldwide climatic shifts. Investigating whether these regional effects propagate to influence broader atmospheric and oceanic circulation patterns is essential for developing holistic climate models.

In summary, this study underscores the importance of volcanic ash deposition as a factor in the albedo and climate dynamics of Antarctica. Given the region's crucial role in regulating global sea levels, further research into these processes is necessary to fully understand the long-term implications of volcanic eruptions on polar environments and the global climate system.

References [Література]

1. Liu, B., Zhao, C., Zhu, L. & Liu, J. (2021). Seasonal changes in arctic cooling after single mega volcanic eruption. *Frontiers in Earth Science* 9: 688250. DOI: <https://doi.org/10.3389/feart.2021.688250>.
2. Fang, S. W., Sigl, M., Toohey, M., Jungclaus, J., Zanchettin, D. & Timmreck, C. (2023). The role of small to moderate volcanic eruptions in the early 19th century climate. *Geophysical Research Letters*, 50(22): e2023GL105307. DOI: <https://doi.org/10.1029/2023GL105307>.
3. Ramaswamy, V., Chanin, M. L., Angell, J., et al. (2001). Stratospheric temperature trends: Observations and model simulations. *Reviews of Geophysics*, 39(1), 71–122. DOI: <https://doi.org/10.1029/1999RG000065>.
4. Gagné, M. E., Kirchmeier-Young, M. C., Gillett, N. P., Fyfe, J. C. (2017). Arctic sea ice response to the eruptions of Agung, El Chichón, and Pinatubo. *Journal of Geophysical Research: Atmospheres*, 122(15), 8071–8078. DOI: <https://doi.org/10.1002/2017JD027038>.
5. Verona, L. S., Wainer, I., Stevenson, S. (2019). Volcanically triggered ocean warming near the Antarctic Peninsula. *Scientific Reports*, 9(1), 9462. DOI: <https://doi.org/10.1038/s41598-019-45190-3>.
6. Yadav, R., Sahu, L. K., Beig, G. & Jaaffrey, S. N. A. (2016). Role of long-range transport and local meteorology in seasonal variation of surface ozone and its precursors at an urban site in India. *Atmospheric Research*, 176, 96–107. DOI: <https://doi.org/10.1016/j.atmosres.2016.02.018>.
7. Malinka, A., Ilkevich, Y., Prikhach, A., et al. (2023). Characteristics of the Snow Cover in East and West Antarctica and Their 20-Year Trends Retrieved from Satellite Remote Sensing Data. *Environmental Sciences Proceedings*, 29(1), 43. DOI: <https://doi.org/10.3390/ECRS2023-15862>.
8. Touzeau, A., Landais, A., Stenni, B., et al. (2016). Acquisition of isotopic composition for surface snow in East Antarctica and the links to climatic parameters. *The Cryosphere*, 10(2), 837–852. DOI: <https://doi.org/10.5194/tc-10-837-2016>.
9. Moran-Zuloaga, D., Merchan-Merchan, W., Rodriguez-Caballero, E., Mulas, M. & Hernick, P. (2024). Long-range transport and microscopy analysis of Sangay volcanic ashes in Ecuador. *Air Quality, Atmosphere & Health*, 17(1), 155–175. DOI: <https://doi.org/10.1007/s11869-023-01434-w>.
10. Ansmann, A., Tesche, M., Groß, S., Freudenthaler, V., Seifert, P., Hiesch, A., & Wiegner M. (2010). The 16 April 2010 major volcanic ash plume over central Europe: EARLINET lidar and AERONET photometer observations at Leipzig and Munich, Germany. *Geophysical Research Letters*, 37(13). DOI: <https://doi.org/10.1029/2010GL043809>.

11. Schäfer, K., Thomas, W., Peters, A., et al. (2011). Influences of the 2010 Eyjafjallajökull volcanic plume on air quality in the northern Alpine region. *Atmospheric Chemistry and Physics*, 11(16), 8555–8575. DOI: <https://doi.org/10.5194/acp-11-8555-2011>.
12. Cole-Dai, J., Mosley-Thompson, E., Thompson, L. G. (1997). Annually resolved southern hemisphere volcanic history from two Antarctic ice cores. *Journal of Geophysical Research: Atmospheres*, 102(D14), 16761–16771. DOI: <https://doi.org/10.1029/97jD01394>.
13. Hildreth, W., Drake, R. E. (1992). Volcán Quizapu, Chilean Andes. *Bulletin of Volcanology*, 54: 93–125. DOI: <https://doi.org/10.1007/BF00278002>.
14. Narcisi, B., Petit, J. R., Delmonte, B., Batanova, V. & Savarino, J. (2019). Multiple sources for tephra from AD 1259 volcanic signal in Antarctic ice cores. *Quaternary Science Reviews*, 210, 164–174. DOI: <https://doi.org/10.1016/j.quascirev.2019.03.005>.
15. Castellano, E., Becagli, S., Hansson, M., et al. (2005). Holocene volcanic history as recorded in the sulfate stratigraphy of the European Project for Ice Coring in Antarctica Dome C (EDC96) ice core. *Journal of Geophysical Research: Atmospheres*, 110, D06114. DOI: <https://doi.org/10.1029/2004jD005259>.
16. Kratzmann, D. J., Carey, S., Scasso, R. & Naranjo, J. A. (2009). Compositional variations and magma mixing in the 1991 eruptions of Hudson volcano, Chile. *Bulletin of Volcanology*, 71, 419–439. DOI: <https://doi.org/10.1007/s00445-008-0234-x>.
17. Solomon, S., Ivy, D. J., Kinnison, D., Mills, M. J., Neely, R. R. & Schmidt, A. (2016). Emergence of healing in the Antarctic ozone layer. *Science*, 353, 269–274. DOI: <https://doi.org/10.1126/science.aae0061>.
18. Stone, K. A., Solomon, S., Kinnison, D. E., et al. (2015). Observing the Impact of Calbuco Volcanic Aerosols on South Polar Ozone Depletion in 2015. *J. Geophys. Res.-Atmos.* 122: 11862–811879. DOI: <https://doi.org/10.1002/2017JD026987>.
19. Ramos, V. A. (2021). Fifty years of plate tectonics in the Central Andes. *Journal of South American Earth Sciences*, 105, 102997. DOI: <https://doi.org/10.1016/j.jsames.2020.102997>.
20. Cembrano, J., Lara, L. (2009). The link between volcanism and tectonics in the southern volcanic zone of the Chilean Andes: A review. *Tectonophysics*, 471(1–2), 96–113. DOI: <https://doi.org/10.1016/j.tecto.2009.02.038>.
21. *Global Volcanism Program* (2013). In: Venzke, E. (Ed.), *Volcanoes of the World*, v. 4.10.5 (27 Jan 2022). Smithsonian Institution. DOI: <https://doi.org/10.5479/si.GVP.VOTW4-2013>. Downloaded 28 Jan 2022.
22. Romero, J. E., Morgavi, D., Arzilli, F., et al. (2016). Eruption dynamics of the 22–23 April 2015 Calbuco Volcano (Southern Chile): Analyses of tephra fall deposits. *Journal of Volcanology and Geothermal Research*, 317, 15–29. DOI: <https://doi.org/10.1016/j.jvolgeores.2016.02.027>.
23. Cabrera, L., Ardid, A., Melchor, I., et al. (2024). Eruption forecasting model for Copahue volcano (southern Andes) using seismic data and machine learning: A joint interpretation with geodetic data (GNSS and InSAR). *Seismol. Res. Lett.*, 95(5), 2595–2610. DOI: <https://doi.org/10.1785/0220240022>.
24. Mastin, L. G., Guffanti, M., Ewert, J. E. & Spiegel, J. (2009). Preliminary spreadsheet of eruption source parameters for volcanoes of the world. US Geological Survey open-file report 1133: 25. URL: <http://pubs.usgs.gov/of/2009/1133/>
25. Qor-el-aïne, A., Béres, A., Géczi, G. (2022). Dust storm simulation over the Sahara Desert (Moroccan and Mauritanian regions) using HYSPLIT. *Atmospheric Science Letters*, 23(4), e1076. DOI: <https://doi.org/10.1002/asl.1076>.
26. Bektaş, S., Lüle, S. Ş. (2022). An integrated method for atmospheric dispersion and corresponding risks: Application to ITU TRIGA Mark II research reactor. *Progress in Nuclear Energy*, 143, 104039. DOI: <https://doi.org/10.1016/j.pnucene.2021.104039>.
27. Li, Y., Tong, D. Q., Ngan, F., et al. (2020). Ensemble PM_{2.5} forecasting during the 2018 camp fire event using the HYSPLIT transport and dispersion model. *Journal of Geophysical Research: Atmospheres*, 125(15), e2020JD032768. DOI: <https://doi.org/10.1029/2020JD032768>.
28. Paez, P. A., Cogliati, M. G., Caselli, A. T. & Monasterio A. M. (2021). An analysis of volcanic SO₂ and ash emissions from Copahue volcano. *Journal of South American Earth Sciences*, 110, 103365. DOI: <https://doi.org/10.1016/j.jsames.2021.103365>.
29. Draxler, R. R., Rolph, G. D. (2010). HYSPLIT (HYbrid Single-Particle Lagrangian Integrated Trajectory) model access via NOAA ARL READY website (<http://ready.arl.noaa.gov/HYSPLIT.php>) NOAA Air Resources Laboratory. *Silver Spring MD*, 25(1).
30. Beres, N. D., Lapuerta, M., Cereceda-Balic, F. & Moosmüller, H. (2020). Snow surface albedo sensitivity to black carbon: Radiative transfer modelling. *Atmosphere*, 11(10), 1077. DOI: <https://doi.org/10.3390/atmos11101077>.
31. Whicker, C. A., Flanner, M. G., Dang, C., Zender, C. S., Cook, J. M. & Gardner, A. S. (2022). SNICAR-ADv4: a physically based radiative transfer model to represent the spectral albedo of glacier ice. *The Cryosphere*, 16(4), 1197–1220. DOI: <https://doi.org/10.5194/tc-16-1197-2022>.
32. Temgoua, F. M., Nguimdo, L. A., & Njomo, D. (2024). Two-Stream Approximation to the Radiative Transfer Equation: A New Improvement and Comparative Accuracy with Existing Methods. *Advances in Atmospheric Sciences*, 41(2), 278–292. DOI: <https://doi.org/10.5194/tc-16-1197-2022>.
33. Warren, S. G. (1982). Optical properties of snow. *Reviews of Geophysics and Space Physics*, 20(1), 67–89. DOI: <https://doi.org/10.1029/RG020i001p00067>.
34. Gardner, A. S., Sharp, M. J. (2010). A review of snow and ice albedo and the development of a new physically based broadband albedo parameterization. *Journal of Geophysical Research: Earth Surface*, 115(F1). DOI: <https://doi.org/10.1029/2009JF001444>.
35. Hansen, J., & Nazarenko, L. (2004). Soot climate forcing via snow and ice albedos. *Proceedings of the National Academy of Sciences*, 101(2), 423–428. DOI: <https://doi.org/10.1073/pnas.2237157100>.

36. Flanner, M. G., Zender, C. S., Randerson, J. T. & Rasch, P. J. (2007). Present-day climate forcing and response from black carbon in snow. *Journal of Geophysical Research: Atmospheres*, 112(D11). DOI: <https://doi.org/10.1029/2006JD008003>.
37. Qu, X., Hall, A. (2007). What controls the strength of snow-albedo feedback? *Journal of Climate*, 20(15), 3971–3981. DOI: <https://doi.org/10.1175/JCLI4186.1>.
38. Doherty, S. J., Warren, S. G., Grenfell, T. C., Clarke, A. D. & Brandt, R. E. (2013). Light-absorbing impurities in Arctic snow. *Atmospheric Chemistry and Physics*, 13(23), 11543–11560. DOI: <https://doi.org/10.5194/acp-13-11543-2013>.
39. Conway, H., Gades, A., & Raymond, C. F. (1996). Albedo of dirty snow during conditions of melt. *Water Resources Research*, 32(6), 1713–1718. DOI: <https://doi.org/10.1029/96WR00712>.
40. Skiles, S. M., Flanner, M., Cook, J. M., Dumont, M. & Painter, T. H. (2018). Radiative forcing by light-absorbing particles in snow. *Nature Climate Change*, 8(11), 964–971. DOI: <https://doi.org/10.1038/s41558-018-0296-5>.
41. Tedesco, M., Doherty, S., Fettweis, X., Alexander, P., Jeyaratnam, J. & Stroeve, J. (2016). The darkening of the Greenland ice sheet: Trends, drivers, and projections (1981–2100). *The Cryosphere*, 10(2): 477–496. DOI: <https://doi.org/10.5194/tc-10-477-2016>.
42. Rignot, E., Mouginot, J., Scheuchl, B., van den Broeke, M., van Wessem, M. J., & Morlighem, M. (2019). Four decades of Antarctic Ice Sheet mass balance from 1979–2017. *Proceedings of the National Academy of Sciences*, 116(4), 1095–1103. DOI: <https://doi.org/10.1073/pnas.1812883116>.
43. Serreze, M. C., Barry, R. G. (2011). Processes and impacts of Arctic amplification: A research synthesis. *Global and Planetary Change*, 77(1–2), 85–96. DOI: <https://doi.org/10.1016/j.gloplacha.2011.03.004>.
44. Bond, T. C., Doherty, S. J., & Fahey, D. W. (2013). Bounding the role of black carbon in the climate system: A scientific assessment. *Journal of Geophysical Research: Atmospheres*, 118(11), 5380–5552. DOI: <https://doi.org/10.1002/jgrd.50171>.
45. Robock, A. (2000). Volcanic eruptions and climate. *Reviews of Geophysics*, 38(2), 191–219. DOI: <https://doi.org/10.1029/1998RG000054>.
46. Schmidt, A., Mills, M. J., Ghan, S., et al. (2018). Volcanic radiative forcing from 1979 to 2015. *Journal of Geophysical Research: Atmospheres*, 123(22), 12491–12508. DOI: <https://doi.org/10.1029/2018JD028776>.

The article was received by the editorial office on 02/22/2025, accepted for publication on 03/05/2026.

Батур М. О.

 0000-0001-9284-8858,

Сельбесоглу М. О.

 0000-0002-1132-3978

Стамбульський технічний університет, Стамбул, Туреччина

Дослідження поширення вулканічного шлейфу і впливу осадження попелу на альbedo снігу в Антарктиді

УДК 551.521.14:551.217.2:551.324.24(99)(045)

Вулканічні виверження є важливим джерелом атмосферних аерозолів, що впливають на глобальний клімат шляхом зміни радіаційного балансу. У віддалених регіонах, таких як Антарктида, вулканічні попелові шлейфи від вивержень у Південній півкулі можуть впливати на альbedo снігу, змінюючи енергетичний баланс регіону. У цій роботі було досліджено поширення вулканічного попелу від південноамериканських вулканів над Антарктидою з використанням моделі HYSPLIT, а також дано аналіз впливу осадження попелу на альbedo снігу за допомогою моделі SNICAR-Adv3. Також в дослідженні було змодельовано різні сценарії вивержень і оцінено, як зміни оптичних властивостей снігу, зокрема альbedo, залежать від різних рівнів осадження вулканічного попелу. Отримані результати демонструють, що осадження попелу є найбільш значимим у нижніх шарах атмосфери (0–4000 м) через гравітаційне осідання і близькість до поверхні, при цьому концентрація частинок у повітрі зменшується з висотою. Встановлено, що альbedo снігу може потенційно зменшуватися приблизно на 1 % внаслідок осадження вулканічного попелу. Результати свідчать про те, що поширення шлейфу та осадження попелу над Антарктидою можливі за певних атмосферних умов, однак ступінь впливу попелу на альbedo суттєво варіює. Така мінливість може призводити до прискореного танення снігу, впливати на кліматичну систему Антарктиди і змінювати регіональний енергетичний баланс.

Ключові слова: Антарктида; антарктичний клімат; альbedo снігу; зміни альbedo; поширення вулканічного попелу; гіпотетичне вулканічне виверження.

Цитування:

Батур М. О., Сельбесоглу М. О. (2026). Дослідження поширення вулканічного шлейфу і впливу осадження попелу на альbedo снігу в Антарктиді. *Український географічний журнал*, 1, 41–54. DOI: <https://doi.org/10.15407/ugz2026.01.041>



Стаття опублікована на умовах відкритого доступу за ліцензією CC BY-NC-ND
<https://creativecommons.org/licenses/by-nc-nd/4.0/>